ADVISE project
FP7-SST-2007-RTD-1 Safety and security by design
GRANT AGREEMENT SCP7-GA-2008-218595

Deliverable D2.8

Draft standard guide for optical deformation measurements in dynamic events

Partners involved: **EMPA, AUK, DD, JRC, UNIL, LTSM-UP**

Authors: **Thorsten Siebert, DD**

Erwin Hack, EMPA

Date: **November 2011**

Draft standard guide for optical deformation measurements in dynamic events

1. Scope

The scope of this document is to provide guidelines for the measurement of a test specimen during a dynamic event by optical full field techniques for deformation measurement. These techniques are capable of measuring the displacement and deformation of an object under dynamic loading by which it is implied that the load can be a harmonic or transient dynamic excitation.

The optical techniques which fulfil these requirements and are mostly used in industrial applications are described in this document:

Digital Image Correlation
Thermoelastic Stress Analysis
Digital Speckle Pattern Interferometry

2. Reference documents

ISO Norms

ISO 11145:2001 Optical instruments – Lasers and laser-related equipment – Vocabulary and symbols.

ISO IEC 17025:2005: "General requirements for the competence of testing and calibration laboratories"

ISO 10012:2003: "Measurement Management Systems - Requirements for measurement processes and measuring equipment"

ISO/IEC Guide 98-3:2008, "Guide to the Expression of Uncertainty in Measurement" (GUM), identical to EN13005:1999: "Guide to the Expression of Uncertainty in Measurement"

ASTM Standards

E 2208-02 Standard Guide for Evaluating Non-Contacting Optical Strain Measurement Systems

C1426-99 Standard practices for verification of calibration of polarimeters. 1999.

3. Symbols

Symbol	Definition	Units
α	coefficient of linear thermal expansion	K^{-1}
$\Delta\phi$	Optical phase shift due to change of displacement	rad
ε	surface emissivity of a material	-
$\boldsymbol{\varepsilon}$	strain tensor	-
θ	illumination angle	rad
λ	wavelength of light	m
ρ	material density	kg m^{-3}
$\sigma_{1,2}$	maximum, minimum principal stress parallel to the surface	N m^{-2}
σ_{kk}	first stress invariant	N m^{-2}
Ψ	Speckle phase	rad
A	calibration factor for TSA	N m^{-2} V^{-1}
c	speed of light (= 3.0 x 10^{8})	ms^{-1}
C_p	specific heat at constant pressure	J kg^{-1} K^{-1}
h	Planck's constant (= 6.63 × 10^{-34})	Js
k	Boltzmann's constant (= 1.38 × 10^{-23})	J K^{-1}
S	signal from the detector	V
T	temperature	K
T_0	ambient temperature	K
$\vec{e}_{Illu}$	unit vector of the illumination beam	-
$\vec{e}_{Obs}$	unit vector of the observation beam	-
d	displacement vector of the surface **d** = (u, v, w)	m
I	intensity of light (irradiance)	Wm^{-2}
I_{obj}	intensity of the object beam	Wm^{-2}
I_{ref}	intensity of the reference beam	Wm^{-2}
i, j	pixel coordinate of a digital image	-
s	sensitivity vector of the DSPI set-up	rad m^{-1}
S	sensitivity matrix of the DSPI set-up	rad m^{-1}
u	displacement in x direction **d** = (u, v, w)	m
v	displacement in y direction **d** = (u, v, w)	m
w	displacement in z direction **d** = (u, v, w)	m

4. Abbreviations and Terminology

2D	Two-dimensional
3D	Three-dimensional
Adiabatic	no heat transfer occurs
Black body	object with ideal emission characteristic
CCD	Charge Coupled Device, a digital camera
DIC	Digital Image Correlation
DL	Digital Level
DSPI	Digital Speckle Pattern Interferometry
ESPI	Electronic Speckle Pattern Interferometry
FFT	Fast Fourier Transform
FOV	Field of View
In-plane	direction parallel to the surface
IR	Infrared
NVH	Noise Vibration Harshness
Out-of-plane	direction perpendicular to a surface
PC	Personal Computer
TSA	Thermoelastic Stress Analysis

5. Principles of the methods

In this chapter the basic principle of the various methods are described in sufficient detail to allow an experiment to be planned.

5.1. Digital Image Correlation

Digital Image Correlation is a data analysis method which is based on digital values of the grey-levels in images of an object. The technique uses mathematical correlation to analyse the grey-level value distribution of the surface of an object in images taken in a temporal series, in general during a mechanical, thermal or other loading of the object. Consecutive images captured during the testing phase will register a change in surface characteristics as the specimen is deformed by the stresses imposed upon it.

Digital Image Correlation (DIC) relies upon the appearance of non-ambiguous digital grey-scale patterns ("fingerprint") of the surface of the object in the images. The technique compares two images acquired at different states, one before and one after some deformation. The two images may be referred to as the reference image (before the deformation) and the deformed image, respectively. After suitable acquisition by a camera, digitised versions of both images are used for analysis.

A sub-image, also called facet, is chosen from the reference image. Starting from an initial estimate of the position and distortion of this facet in the deformed image, the parameters that most accurately represent the transformation of the grey value distribution from the reference image to the other image are determined by using a best-fit matching or correlation algorithm. The interpolation of the intensity distribution in the images enables the determination of the location of a facet with an accuracy of less than 1/100 pixel to be achieved [1 DIC].

Figure 1 represents an example of the transformation of a facet from a reference image to the deformed one. In this case, not just the position, but also the form of the facet has changed. The correlation algorithm needs to be able to handle both types of change or deformation.

Therefore, in general, affine transformations are used to perform the matching of the grey-level distributions between the images. Quality parameters calculated during the correlation, such as the accuracy of the match or remaining residuum, can be used to indicate a valid or non-valid match or correlation [2 DIC, 3 DIC].

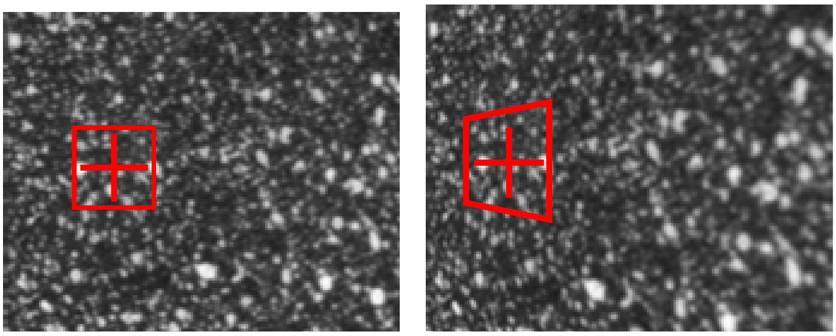

Figure 1; Example of the transformation of a facet between two images.

When a single camera is used then the DIC technique is able to determine displacements in a plane only (2D). In general, both displacements perpendicular to the viewing direction and parallel to the image plane have to be determined [4 DIC, 5 DIC].

The use of two or more cameras allows the measurement of 3D displacements of the object surface. The cameras are arranged in a stereoscopic setup so that the cameras observe the object from different angles. The acquisition of the images by all cameras is synchronized. A facet, representing an area on the surface of the object, is identified in the images from all cameras. Knowledge of the imaging parameters and the position of the cameras in 3D space allows the viewing direction for each pixel of the cameras to be determined. The intersection of the viewing directions of the pixel representing the same object facet determines the position of this surface area on the object. Tracking the position of this facet in a sequence of images for each camera allows the calculation of the 3D displacement of the surface of the object. In figure 2 a stereoscopic setup of two cameras is shown [6 DIC].

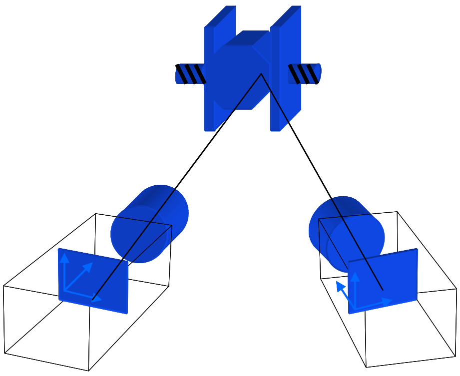

Figure 2: Stereoscopic setup of two cameras for measuring 3D displacements.

For dynamic measurement the use of high-speed cameras is beginning to become routine. Several applications and overviews have been reported [7 DIC, 8 DIC, 9 DIC]

5.2. Thermoelastic Stress Analysis

Thermoelastic Stress Analysis (TSA) is based on the fact that a solid body experiences a temperature variation when strain is induced. In general, the temperature rises in compression and falls in tension. Under elastic and adiabatic conditions, the surface strain can be deduced from measurements of the surface temperature. This involves the use of very sensitive infrared cameras capable of measuring temperature changes down to 0.001°C (1 mK). Adiabatic conditions are achieved when the strain-inducing event is sufficiently fast to prevent significant heat transfer across the field of interest. To achieve adiabatic conditions and a high thermal resolution lock-in techniques are often applied in which cyclic loading is used. The theoretical basis for the technique and the development of its mathematical description can be found in several text-books [1 TSA, 2 TSA, 3 TSA, 4 TSA], and only a simplified outline is presented here.

The application of a sinusoidal load to a solid generates a sinusoidal temperature variation at the same frequency but with a phase different from the load signal. The signal measured by the detector is usually related to the first stress invariant on the surface of the solid, although strictly the surface temperature is related to the first strain invariant. It can be shown that

$$\Delta T = -T_0 \frac{\alpha}{\rho C_p} \sum \Delta\sigma_{kk} \qquad (1)$$

where ΔT is the amplitude of the temperature variation measured by the detector, T_0 is the ambient temperature of the test, α is the coefficient of linear thermal expansion, ρ is the material density, C_p the specific heat at constant pressure and $\sum \Delta\sigma_{kk}$ is the first stress invariant. The ratio $\frac{\alpha}{\rho C_p}$ is known as the thermoelastic constant. Equation (1) is valid for homogeneous isotropic materials undergoing elastic and adiabatic transformations. Because of the minute temperature changes involved it can be safely assumed that the elastic and thermal properties are constant with respect to temperature. In practice the following inverted form is employed to retrieve the sum of principal surface stresses:

$$\Delta(\sigma_1 + \sigma_2) = A\,S \qquad (2)$$

where A is the calibration factor and S the signal from the detector.
For TSA or measurement of other transient temperatures high-speed cameras are often used [5 TSA].

5.3. Digital Speckle Pattern Interferometry

Digital Speckle Pattern Interferometry (DSPI) was formerly known as Electronic Speckle Pattern Interferometry (ESPI) [1 DSPI; 2 DSPI; 3 DSPI]. DSPI employs laser light to measure the surface deformation of an object in all directions, in-plane and out-of-plane. Full-field information about 3D-displacement vectors is obtained when the specimen is illuminated from different directions, see Figure 3.

The object from which the laser light scatters back is imaged by a camera. The object light is superimposed on a static reference wave such that at every camera pixel *(i,j)*, i.e. in every surface location, the phase difference of reference and object light is measured with interferometric resolution.

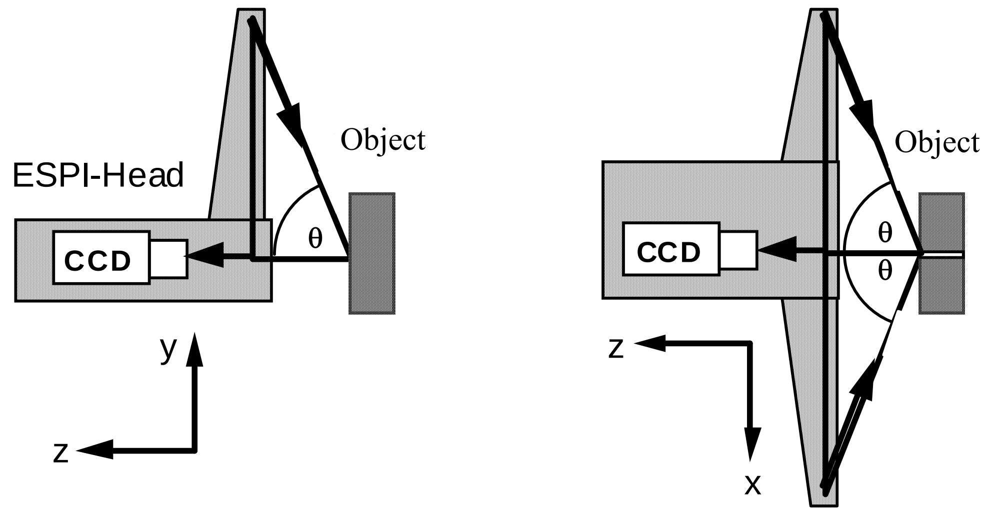

Figure 3: Schematic of the illumination of an object and definition of the axes for 3D-DSPI where CCD: camera; θ: illumination angle w.r.t. the camera axis.

When the object is deformed, the length of the object path changes. The change of optical path length results in a change $\Delta\phi(i,j)$ of the relative optical phase of the two beams and therefore changes the intensity of the speckles. The intensity at a pixel of the CCD camera is

$$I(i,j) = I_{obj}(i,j) + I_{ref}(i,j) + 2\sqrt{I_{ob}(i,j) \cdot I_{ref}(i,j)} \cdot \cos(\Psi(i,j) + \Delta\phi(i,j)) \quad (3)$$

where $I(i,j)$ is the intensity at the pixel (i,j), I_{obj} and I_{ref} are the intensities of the object beam and the reference beam, Ψ is the stochastic phase between the reference and the object beam, and $\Delta\phi$ is the optical phase change due to the deformation. From the corresponding change of the interference pattern the displacement of the object surface element is inferred. The relation between phase and displacement field is given by

$$\Delta\phi(i,j) = \mathbf{s}(i,j) \cdot \mathbf{d}(i,j) \quad (4)$$

$$\mathbf{d}(i,j) = \begin{pmatrix} u(i,j) \\ v(i,j) \\ w(i,j) \end{pmatrix} \text{ and } \mathbf{s}(i,j) = \frac{2\pi}{\lambda}\left[\mathbf{e}_{Obs}(i,j) - \mathbf{e}_{Illu}(i,j)\right] \quad (5)$$

d(i,j) is the displacement of the surface of the object at the point imaged onto pixel (i,j), **s** is the sensitivity vector of the optical set-up, which is determined by the direction of illumination of the object point and the observation direction. $\mathbf{e}_{Illu}(i,j)$ and $\mathbf{e}_{Obs}(i,j)$ are the unit vectors of the respective directions. The displacement vector, **d,** cannot be calculated from a single measured intensity I(i,j). The measurement of all three components of displacement vector requires a minimum of three sensitivity vectors. These can be created by three linearly independent illumination directions (Figure 3) or a mix of out-of-plane illuminations and in-plane illuminations. When the three sensitivity vectors are combined into a matrix, the displacement can be retrieved by inversion of Eq.(4).

$$\mathbf{d}(i,j) = \mathbf{S}^{-1}(i,j)\,\mathbf{\Delta\varphi}(i,j) \quad (6)$$

where the vector $\mathbf{\Delta\varphi}(i,j)$ combines the three total phase changes for the three illumination directions.

In order to extract the phase from the intensity expression in Eq.(3) we must eliminate the two intensities $I_{obj}(i,j)$ and $I_{ref}(i,j)$ and the random initial speckle phase Ψ. From a minimum of three images with controlled additional steps in the phase, the phase $\Delta\varphi(i,j)$ can be obtained. A common method uses four images with a phase step of 90° between. The change of optical phase for a static load case is then determined as

$$\Delta\phi = \arctan\frac{I_4 - I_2}{I_1 - I_3}\bigg|_{after\ load} - \arctan\frac{I_4 - I_2}{I_1 - I_3}\bigg|_{before\ load} \tag{7}$$

Due to the trigonometric function the optical phase, $\Delta\varphi$, can be determined only modulo 2π (wrapped phase). Before the calculation of the displacement the optical phase has to be unwrapped and the absolute order of the fringe has to be found. While the principle described so far is applicable to static deformations, for dynamic experiments there are related extended techniques, i.e.,

1. **Time average technique.** This technique is used to identify mode shapes of vibrating surfaces. A sinusoidal load is applied and the interference signal is integrated during the frame acquisition time. It can be shown that there is a set of fringes given by the zeroes of a Bessel-function [4 DSPI]. For further evaluation, the map of the contrast of the fringes exhibit normally better quality than the difference intensity of vibrating and static surface.

2. **Stroboscopic technique.** This technique is used to quantify periodic deformations. A sinusoidal load is applied, and the illumination is chopped synchronously with the excitation. The camera then sees a frozen movement which can be evaluated like a static deformation, applying Eq.(7) to the difference of the object in rest and the vibrating object. Note that the maximum of the vibration amplitude can be shifted w.r.t. the maximum of the excitation force. At resonance, e.g., this shift is 90°.

3. **Real-time methods**. For transient loading, there is no time to acquire phase-stepped images in sequence; the phase should be evaluated from a single frame. To achieve this, carrier fringe methods have been introduced which optically generate a carrier fringe by tilting the reference wave w.r.t. the object wave, and the evaluation of the phase is done with a FFT technique.

   Other techniques use special set-ups [5 DSPI, 6 DSPI], e.g. splitting a single interferogram optically into four and using polarization elements to obtain four phase-stepped frames in parallel. These can again be treated like the static case, applying Eq.(7) after the test.

The first two techniques apply to periodic deformations, such as vibrations and resonance experiments. In the first case, the frequency must be much higher than the camera frame rate.

6. Apparatus

The techniques are image based, and cameras are required. For the measurement of dynamic events, the cameras need to be able to acquire the images at a suitable frame-rate in order to achieve a sufficient temporal resolution of the event. The combination of illumination and camera should be able to operate with an exposure time that causes no blurring of the object during the acquisition of the images. Depending on the technique, special timing and triggering control might be required to synchronize the acquisition of the cameras and/or the event.
In the following, the methodologies for the application of the techniques are discussed in sufficient detail to allow an experiment to be planned. However, reference to manufacturers' instructions is necessary for the execution of the experiment.

6.1. Digital Image Correlation

The standard configuration for a DIC setup consists of the following elements:

- Digital cameras;
- Imaging optics;
- Illumination light source;
- PC and control electronics for image acquisition;
- Sample with loading apparatus.

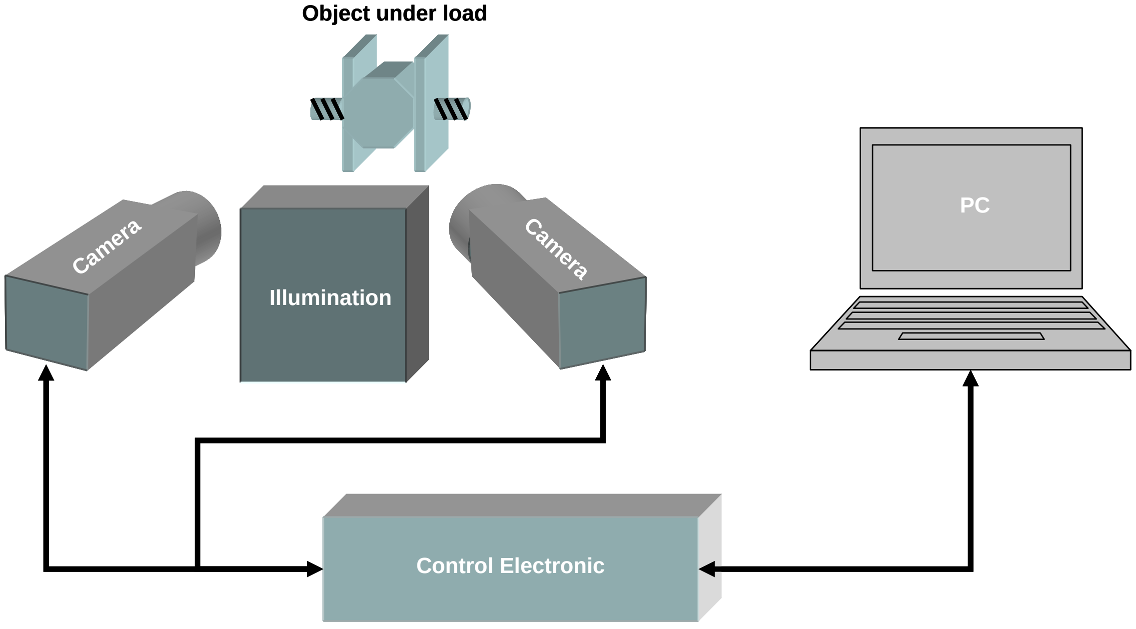

Figure 4: Schematic of a digital image correlation apparatus for 3D measurement.

To illuminate the surface of the object white light or monochromatic light can be used. Appropriate matched lenses are employed to create an image of the object on the camera sensors. The data are transferred via control electronics to a computer. This control unit can be separate or part of the computer itself. The computer controls the image acquisition, stores the data and performs the evaluation and visualization of the results.
For dynamic events, the maximum frame rate of the cameras limits the maximum speed of the displacement which can be analysed. In general the frame rate of the cameras should be at least twice the highest frequency component which is to be analysed.

6.2. Thermoelastic Stress Analysis

The standard configuration for a TSA setup consists of the following elements:

- Thermal detector (infrared camera);
- Imaging optics;
- Sample with loading apparatus;
- PC and control electronics for image acquisition and load control.

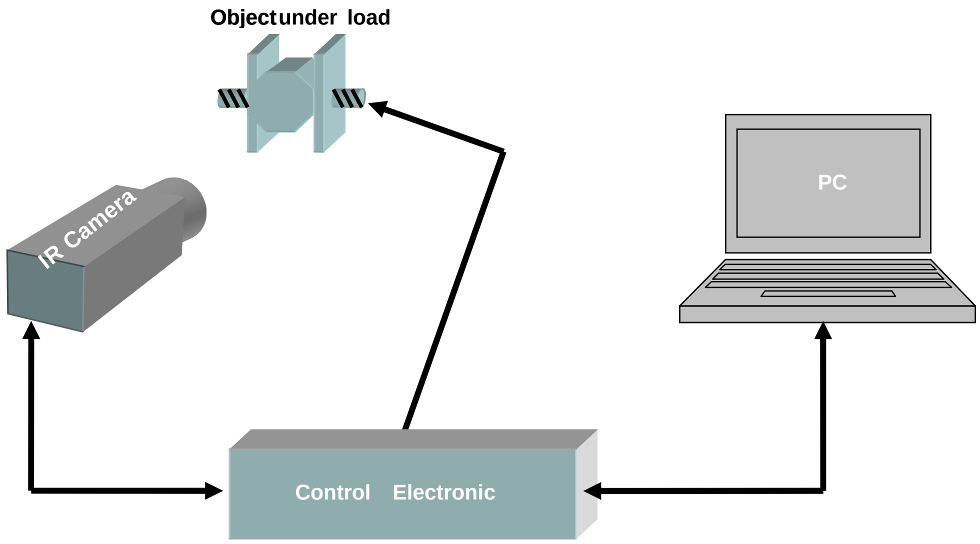

Figure 5: Schematic of a TSA apparatus for measurement of surface stress.

The key component for thermoelastic stress analysis is a detector capable of measuring small temperature changes down to 1 mK on the surface of the object under load. Commercial instruments are available and operate either in the 8–12 µm wavelength range of IR radiation (MCT, mercury-doped cadium-telluride photovoltaic photon detector), or the 3–5 µm range (InSb detector arrays). Array detectors feature typically 240x360 pixels. It is recommended to use cooled detectors with a noise-equivalent temperature difference of 25 mK or less in order to achieve the high resolution necessary for TSA.

The signal from the detector is usually noisy and so extraction of the required information requires signal processing. The most common approach is to use a lock-in amplifier to which the inputs are the detector output and a reference signal related to the applied excitation of the object. An alternative approach is to use a fast Fourier transform and digital signal processing, which offers the possibility of analysing the strain generated by variable amplitude loads. Commercial systems for TSA include the lock-in electronics and evaluation software for periodic temperature signals. The first apparatus of the market was SPATE [6 TSA,7 TSA], but today there are other systems such as DELTATHERM or FLIR.

For dynamic events, some systems are limited by the maximum frame rate of the camera, because they acquire frames within a single cycle of the loading. Hence, the load period should cover at least three frame periods. In general the frame rate should be at least twice the loading frequency. Other systems can accommodate higher loading frequencies by aliasing the camera frame rate with the cycles of the loading.

6.3. Speckle Pattern Interferometry

The standard configuration for a DSPI setup consists of the following elements:

- Laser light source;
- Digital camera;
- Illumination and imaging optics;
- Phase stepping unit (e.g. piezo element activated mirror);
- PC and control electronics for switching the illumination direction, phase stepping and image acquisition;
- Sample with loading device.

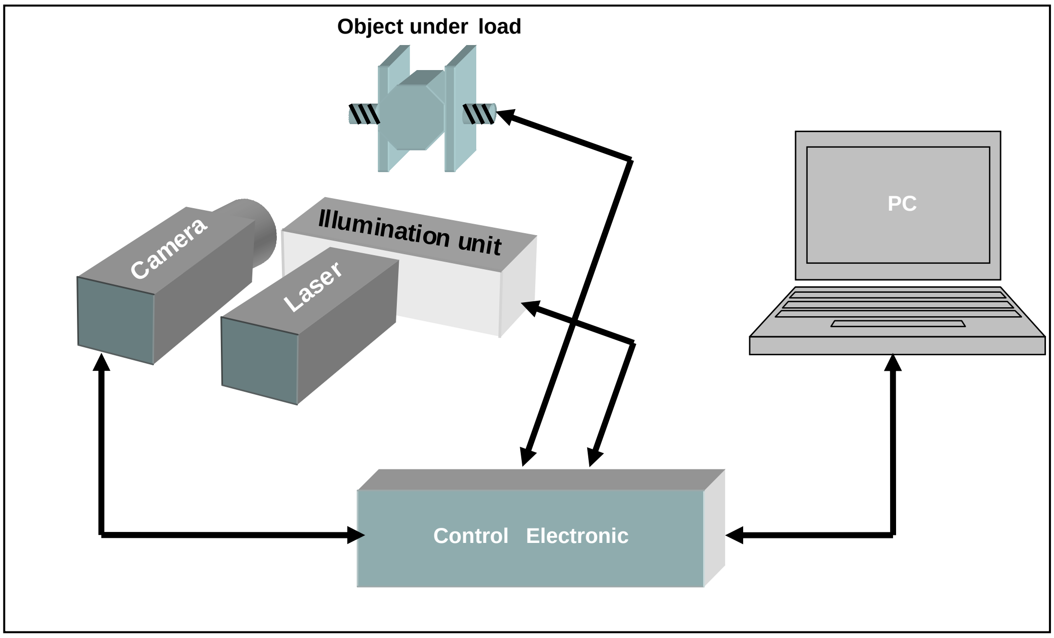

Figure 6: Schematic of a DSPI apparatus for 3D measurement.

For dynamic measurements the following element can be added:

- Stroboscope (e.g. chopper wheel, acousto-optic modulator, electro-optic shutter).

For time average methods, the loading frequency must be at least four times the frame rate, but is limited in the high frequency range only by the decreasing vibration amplitude. Stroboscopic systems are limited by the frequency of the stroboscopic unit and the duty cycle of the illumination which should remain well below 50%. Finally, real-time methods are limited by the maximum frame rate of the camera and the number of fringes generated between two frames.

7. Sample preparation

Since these techniques rely on images there may be special requirements for the preparation of surface of the measured object, which are dependent on the technique employed. In general, it is necessary to avoid direct reflections of the illumination because this will cause glare and create areas where it might not be possible to perform the analysis. On the other hand, the image should use as much as possible of the dynamic range of the camera, in order to achieve the best signal-to-noise ratio. The specific requirements for the individual techniques are described below.

7.1. Digital Image Correlation

The digital image correlation technique relies on the appearance of a non-ambiguous grey-level value distribution (or "fingerprint") in the image of the camera. For an optimized correlation, the features should have a size of 2-3 pixels in the image, and within a facet the pattern should include grey-level gradients in every direction [4 DIC].

In an application using only one camera for a 2D setup, the texture of the object surface, such as roughness or scratches, in combination with the illumination might be able to generate suitable features. For a 3D measurement, in general, the surface texture of the object does not provide the necessary conditions in the images. Therefore, the surface needs to be prepared in a way that the object surface shows an appropriate grey-level value distribution in the images. Various methods for generating the surface texture on the object can be used, depending on the texture of the object, the required feature size on the surface of the object, the type of loading which is to be applied and the resulting deformations of the object.

The most common way is the use of matt white and black paint. These can be applied by the use of air brush systems or spray cans to achieve a homogenous matt background with matt speckled dots on top. In general, to achieve the best contrast black and white colours are used. Depending on the colour of the original texture and colour of the illumination light also other combinations of colours are possible. For larger areas the dots can be generated by using a stamp or similar device.

Another means of surface preparation is to print a synthetically generated pattern onto an elastic foil and to stick this foil onto the surface of the object. When using this method, it is necessary to ensure that the foil can be attached fully to the surface and that the foil is flexible enough to follow the deformations of the surface of the object without influencing their behaviour.

Regardless of the surface preparation method, a reflection of the illumination in any images of the cameras needs to be avoided.

7.2. Thermoelastic Stress Analysis

Since all solids exhibit the thermoelastic effect, the technique can be used directly on most components. A surface emissivity of more than $\varepsilon = 0.9$ is recommended approximating a black body ($\varepsilon = 1$) to maximize the thermal radiation and hence the signal. A uniform surface finish is required. The use of sandblasting, a thin coating of the order of 20 µm of matt black paint, or a powder sprayed onto metallic shiny surfaces increases the emissivity and improves surface homogeneity. However the coating can cause attenuation of the photon signal at very high frequencies or with thick coatings when the coating begins to act as a strain witness. Typically, two passes with an aerosol spray is sufficient to provide a uniform coating and will not have any deleterious effect at frequencies in the range of 5 to 30Hz.

7.3. Speckle Pattern Interferometry

The surface of the sample has to be rough in order to obtain a diffuse scattering of the laser beam. The roughness r_a should be larger than $\lambda/4$. In the case of a low roughness, a highly reflecting surface, or a transparent object, a bright paint or powder has to be applied to the surface. However, care must be taken that the layer will deform like the underlying surface without reinforcing it.

8. Calibration procedure

In order to obtain accurate measurements, for each technique it is required to have knowledge of certain parameters or factors that describe the actual measurement setup. This chapter explains which parameter or factors are essential for the techniques and how they can be determined.

Once the system has been calibrated through the determination of parameters, a calibration of its performance based on the use of defined strain and/or deformation fields is recommended to obtain traceable measurement results through direct calibration. For static strain measurements, a SPOTS reference material is available (see www.opticalstrain.org)[1] while for dynamic measurements, reference materials are under development (see www.dynamicvalidation.org)[2].

8.1. Digital Image Correlation

Calibration of a digital image correlation system requires the determination of the imaging or projection parameter of each camera (intrinsic parameter).

In general the description of the imaging process is based on the pin-hole model. This can be described by the focal length and the position of the optical axis in the image plane, the so called principle point. In addition, distortion parameters are used to describe the imaging better. Figure 4 illustrates the pin-hole model and its parameters [10 DIC].

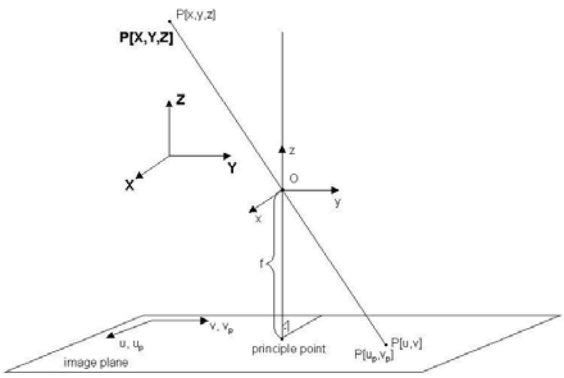

Figure 4: Schematic of the pin-hole model for imaging.

A second set of parameters is required, which are extrinsic parameters that define the position of each imaging sensor relative to a global coordinate system. Both sets of parameter need to be calculated for each setup or each time the imaging arrangement of a DIC system is changed.

The intrinsic and extrinsic parameters are calculated from images of a known pattern. This pattern can be a set of dots or squares with a defined distance or length on a plane target. By

[1] E. Patterson, E. Hack, P. Brailly, R. Burguete, Q. Salem, T. Siebert, R. Tomlinson, M. Whelan, *Calibration and evaluation of optical systems for full-field strain measurement*, Opt. Las. Eng. **45** (2007) 550–564

[2] Davighi, A.; Burguete, A.; Feligiotti, M.; Hack, E.; James, S.; Patterson, E., "The development of a reference material for calibration of full-field optical measurement systems for dynamic deformation measurements", Applied Mechanics and Materials Vol. 70 (2011) 33-38

acquiring a series of images at different positions and orientations of the target in front of the cameras, using a bundle adjustment algorithm, the imaging parameters and the extrinsic parameters of all the cameras can be calculated.

In general, the entire camera sensor should be used for the calculation of the projection parameter even if only a reduced area is used for the measurement itself.

8.2. Thermoelastic Stress Analysis

A calibration can be performed experimentally to determine the thermoelastic constant for the actual experiment [8 TSA]. Or it can be computed based on knowledge of experimental conditions and material properties. Normally, the detector is calibrated for temperature measurements so that the calibration curve S(T) is known.

Experimental calibration of TSA data can then be achieved using a calibration specimen of known geometry such as a beam subject to four-point bending, or a disc subject to compression across a diameter or a tensile strip. The exact circumstances of the component test must be reproduced including temperature, frequency, and coating thickness as well as material properties. These conditions are often difficult to achieve and can be avoided by bonding an isopachic strain gauge to the test specimen in order to realise a direct calibration constant. The location of the gauge should be an area of approximately uniform stress so that the errors from the gauge are minimised and an area is provided on and around the gauge from which a thermoelastic measurement can be taken. Since the gauge will generate heat when used, the strain gauge and temperature measurements should not be made simultaneously.

8.3. Speckle Pattern Interferometry

For quantitative evaluations of displacement, the sensitivity vectors and the magnification of the optics should be known or measured. The calibration of the optical magnification is done by taking an image of an object of known dimension in the object plane of the camera, and associating the pixels on the camera to appropriate points on the object. The sensitivity vectors can be determined by measuring the position of the illuminating point sources, the observation direction, and the surface coordinates of the object.

The verification of these calibrations can be achieved experimentally by a calibration specimen of known geometry such as a turntable under rotation, a beam subject to four-point bending, a disc subject to compression across the diameter, or a tensile strip.

The wavelength of gas and solid-state lasers do not have to be calibrated. For diode lasers, the wavelength may be tunable and therefore the use of a calibration curve of the wavelength in terms of operation current and temperature is advisable.

9. Measurement and recording procedures

This chapter describes the generic procedure for the acquisition of the data required for each technique. Starting with the setup of the measurement device and ending with the storage of data. The methodology is discussed in sufficient detail to allow an experiment to be performed. However, reference to manufacturers' instructions maybe necessary for the execution of the experiment.

9.1. Digital Image Correlation

The preparation of a DIC system for a measurement is described in the following steps:
Mechanical setup of system:

- Make sure that the cameras are on a rigid support;
- The area of interest of the object needs to be in field of view of the cameras;
- The area of interest should fill the image as much as possible ;
- The angle between the cameras should be in a range of 30° to 60°;
- Make sure that the cameras are fixed tightly in position;
- Prepare the surface of the object with a suitable speckle pattern.

Optical setup of DIC system:

- Adjust the focusing of the lenses at the centre of the images with the aperture open;
- Close the aperture in order to get a sufficient depth of focus;
- Adjust the illumination to achieve the brightest possible image but avoiding any reflections in the field of measurement;
- Set the exposure time to use most of the dynamic range of the cameras. For dynamic events avoid any blurring of the object during the exposure time.

Determination of projection parameters:

- Select a calibration target that fills most of the field of view;
- Acquire a series of simultaneously captured images with the cameras of the calibration target at different orientations;
- Calculate the intrinsic and extrinsic parameters for the cameras.

Recording of images:

- Check if the required area of interest on the surface of the object can be correlated in an appropriate way. For this check, acquire images of the object without loading and perform an evaluation.
- Set an appropriate recording mode in order to capture the displacement of the object during the loading in an appropriate rate.
- Start the acquisition and store the images on a hard disk.

9.2. Thermoelastic Stress Analysis

The preparation of a TSA system for a measurement is described in the following steps:

Mechanical setup of the experiment:

- Prepare the specimen surface if necessary;
- Insert the specimen into the loading system;
- Position the infrared camera to view the area of interest on the specimen;
- Make sure that the camera is fixed tightly in position.

Setup of TSA system:

- Adjust the focusing of the lens;
- Avoid reflections of near-by objects with different temperatures (including the operator him/herself);
- Choose the temperature range and calibration suited for the experiment;
- Determine the frequency for the lock-in experiment based on the material, specimen geometry and loading condition to achieve adiabatic conditions;
- If necessary, perform a strain-calibration using a reference material or a strain gauge.

Recording of images:

- Set an appropriate recording mode in order to capture the temperature evolution of the object during the loading with the appropriate rate;
- Start the acquisition and store the resulting amplitude images on a hard disk.

The reliability and accuracy of TSA is dependent on achieving adiabatic conditions during cyclic loading. The minimum frequency at which this can be achieved is dependent on the thermal conductivity of the material and the gradients in the stress distribution being examined. Most metals behave adiabatically above 2 Hz but concerns about stress concentrations, coating effects and system electronics lead to typical testing frequencies in the range of 5 to 20 Hz. Compliance with adiabaticity can be checked by either increasing the frequency from 1Hz until convergence to a constant signal is achieved, or by examining the phase of the temperature relative to the excitation signal. Non-adiabatic behaviour creates an observable phase shift.

9.3. Speckle Pattern Interferometry

For the set-up of DSPI experiments a vibration-isolated table is recommended.

Mechanical setup of the experiment:

- Prepare the specimen surface if necessary;
- Insert the specimen into the loading system;
- Make sure that the DSPI sensor is fixed tightly in position;
- Ensure that no relative movement of the sensor with respect to the sample occurs;
- Avoid vibrations and air flows.

Setup of DSPI system:

- Align the sample and the optical system. The optical axis should be perpendicular to the surface.
- Focus the camera on the area of interest on the specimen;
- Determine the magnification of the imaging system and the sensitivity matrix;
- Adjust the intensity of the laser light illumination for all illumination directions;
- For stroboscopic method: choose the duty cycle and increase the illumination correspondingly.
- Adjust the reference beam intensity to obtain good contrast of fringes without extensive saturation of the camera. Due to the speckle effect, some 5% of the pixels may be saturated.

Recording of images:

- Acquire a set of phase-stepped images of the reference state of the object;
- Increase the load level and ensure that the fringe density is not too high;

- Time-average method: Acquire a set of phase-stepped images of the vibrating object; calculate and store the contrast image
- Stroboscopic method: Acquire a set of phase-stepped images of the vibrating object; repeat with different phase lag w.r.t. the excitation signal to obtain the maximum deformation.
- Repeat the procedure if necessary for different frequencies.
- Store the images.

The outcomes of a stroboscopic procedure are phase maps which are the raw data in the evaluation process to follow. In time-average and real-time procedures the raw data are intensity distributions.

10. Data processing procedures

The procedure to determine required measurement results from the acquired information is the topic of this chapter. The individual steps describing the path of evaluation with respect to the use of these techniques for dynamic events are identified. The methodology for the data processing is discussed. However, reference to manufacturers' software instructions maybe necessary for the interpretation of the results.

10.1. Digital Image Correlation

Select the series of images to be evaluated:

- Select the images from the series to be analysed;
- Select the projection parameter which belongs to the setup during the acquisition of the images.

Define the correlation parameter:

- Set the size of the facet;
- Set the distance between the centres of two neighbour facets;
- Define the quality parameter for a valid correlation;
- Select a reference camera and reference step.

Select a starting point:

- Select one point and the surrounding facet in the reference step of the reference camera;
- Perform a correlation for this facet between the cameras in the reference step;
- Perform a correlation for this facet between the images of the series from each camera.

Perform a full field evaluation:

- Beginning from the start point, perform a full-field correlation between the images of the cameras in the reference step;
- Beginning from the start point, perform a full-field correlation between the images of the series from each camera.

Reconstruct the object surface:

- Reconstruct for each valid correlated facet the coordinate of the corresponding object point at the reference step;
- Determine from the changes of the positions of the facets within the image series the changes of the coordinate of the corresponding object point at each measurement step and calculate the contour of the object surface at this measurement step;

- Define a suitable coordinate system.

Calculate deformations:

- Define a reference step;
- Calculate the difference of the coordinates of a facet between the reference and the any other step.

Visualization and extraction of data:

- Display the reconstructed object surface and/or deformation in a suitable way;
- Select points, lines or areas on the reconstructed object surface;
- Extract the required quantity for each selection over the measurement steps;
- Perform frequency analysis techniques or similar methods to determine the required information;
- Display or export the extracted data in a suitable way.

10.2. Thermoelastic Stress Analysis

Data processing is usually provided by the software accompanying the instrumentation and involves correlating the signal from the detector with the forcing signal and calibrating it based on expression (2). Separation of the stress invariant to provide the individual principal stresses can be achieved in a number of ways which have been reviewed by Stanley and Dulieu-Smith [9 TSA] and by Barone and Patterson [10 TSA].

10.3. Speckle Pattern Interferometry

In time-average methods there is no further analysis necessary. The contrast image is the outcome. The outcomes of a stroboscopic procedure with temporal phase stepping are wrapped phase maps. In real-time procedures either a phase-stepping method must be undertaken from the phase-stepped sub-images, or the interference pattern with the carrier fringes (spatial phase shifting) must be analyzed using a Fourier method.

Once the wrapped phase map is obtained, an unwrapping algorithm is applied to generate a continuous map of the phase. The knowledge of a point with zero deformation inside the FOV allows the determination of the absolute value of the phases from which the displacement field **d** can be obtained by applying the inverse of the sensitivity matrix, Eq.(6).

In order to obtain strain maps, the in-plane displacement fields are numerically differentiated. The elements of the strain tensor **ε** are calculated from the displacement field as spatial derivatives:

$$\boldsymbol{\varepsilon}(i,j)=\begin{pmatrix} \frac{\partial u(i,j)}{\partial x} & \frac{1}{2}\frac{\partial v(i,j)}{\partial x}+\frac{1}{2}\frac{\partial u(i,j)}{\partial y} & \frac{\partial w(i,j)}{\partial x} \\ \frac{1}{2}\frac{\partial v(i,j)}{\partial x}+\frac{1}{2}\frac{\partial u(i,j)}{\partial y} & \frac{\partial v(i,j)}{\partial y} & \frac{\partial w(i,j)}{\partial y} \\ \mathrm{NA} & \mathrm{NA} & \mathrm{NA} \end{pmatrix} \tag{8}$$

In the case of curved objects the local surface normal has to be taken into account at every measuring point to correct for the viewing angle when calculating in-plane strains.

11. Areas of applications

Applications of DSPI and DIC abound and include static, quasi-static and dynamic analyses. TSA has also been used on static problems, e.g. on the assessment of residual stresses [11 TSA,12 TSA]. The use of TSA to evaluate stress intensity factors associated with fatigue cracks has been reported [13 TSA], and is beginning to be performed routinely. Similar is true for DIC [11 DIC].

The need for the measurement of deformation and strain in dynamic events is particularly important in the field of transportation. This area has a high potential for the use of optical full-field measurement techniques. The applications are categorised by the kind of dynamic event in the following. The excitation of an object or component by a single frequency is more common in the R&D area where the principal behaviours are subject of interest. The comparison of the resonance frequencies and corresponding mode shapes is of special interest here.

Similar results can be achieved by the use of noise excitation or operating vibrations which excite many frequencies simultaneously. The advantage here is that the resonance frequencies can be unknown and with one measurement several eigenmodes are found. For separation of the eigenfrequencies and modes, spatial frequency analysis methods can be used.

Another common approach is the excitation by a shock event. This method is also applicable for studies on eigenfrequencies and modes.

Finally, the investigation of impacts on objects or components as they occur e.g. in crash testing of vehicles is of major importance for the transportation industry.

In the following section several applications of the different techniques in the fields of ground transportation are shown to illustrate a variety of uses and the importance of the results. In the scientific literature many more examples for these applications can be found.

11.1. Determination of material properties

Many materials show a dependency of their properties in time. Besides aging and humidity effects, metal material and composite materials have a strong dependency of their behaviour on the strain rate. Therefore the use of optical techniques is important to get knowledge of these time dependency to allow a better prediction and simulation of these materials e.g. for crash or impact test [12 DIC]. A general treatment of the subject is given in [13 DIC, 14 DIC].
Non-homogeneous and non-isotropic material like fibre composites are challenging for non full field techniques. Here the application of DIC and TSA allow a better understanding of the material behaviour and properties [14 TSA, 15 TSA].

11.2. Mode shape analysis

The knowledge of the mode shape of single components or complex structures has a big impact for the estimation of life-time and in the field of Noise Vibration Harshness (NVH). Here the optical full-field measurement techniques have advantages as they allow the measurement of large areas with high spatial resolution without changing the properties of the object by e.g. adding masses or changing of the material properties.
Here the techniques measuring the displacement (DIC, DSPI) are predominantly used although TSA can give mode shapes in cases where the stress levels are appreciable. The technique and configuration to be most suitable depends on the frequency and amplitude range as well on the dimensions of the field of measurement [10 DIC, 15 DIC,16 DIC 17 DIC].

11.3. Impact event

High-speed measurements are needed when experiments using impact testing are performed. Presently, DIC is the most appropriate method when it comes to large deformations. However, sometimes – and mostly in reality – no measurements are taken during an impacting event, but the full-field optical methods offer a means for off-line, post-impact analysis. When a comparison to the data from an undamaged structure is available [7 DSPI], residual life estimation comes into the reach of the analyst. This field of damage assessment [8 DSPI] is particularly important for aircraft industry.

11.4. Validation of numerical analyses

Full-field techniques are especially useful in the validation of simulations, because they offer data-rich fields that can be compared to the outcome of a numerical analysis. This is especially important for the simulation of impact damage [18 DIC], although the principle of comparing data rich maps is a generic task.

12. Bibliography

12.1. DIC

1 DIC Becker Th., Splitthof K., Siebert Th., Kletting P., "Error Estimations of 3D Digital Image Correlation Measurements", Proc. SPIE Vol. 6341, 63410F (2006)

2 DIC Lecompte D., Sol H, Vantomme J, Habraken A., "Analysis of speckle patterns for deformation measurements by digital image correlation", Speckle06, SPIE Vol. 6341, 63410E, (2006)

3 DIC Siebert T., Becker T., Splitthof K., Neumann I., Krupka R., "High-speed digital image correlation: Error estimations and applications", Optical Engineering, 46(5):051004 (2007)

4 DIC Sutton M.A., Orteu J-J., Schreier H.W., „Image Correlation for Shape, Motion and Deformation Measurements", Springer Science+Business Media, LLC, ISBN 978-0-387-78746-6 (2009)

5 DIC Pan B., Qian K., Xie H., Asundi A., "Two-dimensional digital image correlation for in-plane displacement and strain measurement: a review", Meas. Sci. Technol. 2009, 20 062001 (17pp)

6 DIC Sutton M.A., McNeil S.R., Helm J.D., Chao Y.J, "Advances in 2-D and 3-D computer vision for shape and deformation measurements", in Photomechanics, P.K. Rastogi, Ed. Topics in Applied Physics, 77, 323-372, Springer Verlag, New York (2000)

7 DIC Schmidt T., Tyson J., Galanulis K., Revilock D., Melis M., "Full-field dynamic deformation and strain measurements using high-speed digital cameras", 26th International Congress on High-Speed Photography and Photonics, SPIE Vol. 5580, 174-185, (2005)

8 DIC Tyson J., Schmidt T., Galanulis K., "3D Image Correlation: Measuring Displacement and Surface Strain", Sensors Magazine, June 2007

9 DIC Reu P.L., Miller T.J., "The application of high-speed digital image correlation", Journal of Strain Analysis for Engineering Design, 2008, 43(8), p. 673-688

10 DIC Yoneyama, S., Kikuta, H. (2006), "Lens distortion correction for digital image correlation.", Opt. Eng. 45(2)

11 DIC Rannou, J., Limodin, N., Réthoré, J., Gravouil, A., Ludwig, W., Baïetto-Dubourg, M.-C., Buffière, J.-Y., Combescure, A., Hild, F., and Roux, S., "Three dimensional experimental and numerical multiscale analysis of a fatigue crack", Comp. Meth. Appl. Mech. Eng., 199 (2010) 1307–1325

12 DIC Moulart R., Pierron F., Hallett S., Wisnom M., "Full-field strain measurements at high strain rate on notched composites tested with a tensile Hopkinson bar", Annual SEM conference, 1-4 June 2009, Albuquerque (NM), USA

13 DIC Avril, S., Bonnet, M., Bretelle, A.-S., Grédiac, M., Hild, F., Ienny, P., Latourte, F., Lemosse, D., Pagano, S., Pagnacco, E., and Pierron, F. (2008) Overview of identification methods of mechanical parameters based on full-field measurements. Exp. Mech., 48, (4), 381–402.

14 DIC Hild, F. and Roux, S. Digital image correlation: from measurement to identification of elastic properties – A review. Strain, 42 (2006) 69–80.

15 DIC Siebert, Th., Wood, R., Splitthof, K., "High Speed Image Correlation for Vibration Analysis", Journal of Physics: Conference Series 181 (2009) 012064, doi:10.1088/1742-6596/181/1/012064

16 DIC Wang, W., Mottershead, J. E., Ihle, A., Siebert, Th., Schubach; H. R., "Finite Element Model Updating From Full-Field Vibration Measurement Using Digital Image Correlation", Journal of Sound and Vibration 330 (2011) 1599–1620

17 DIC Siebert, Th., Wang W., Mottershead J.E., Pipino A., "Application of High Speed Image Correlation for Measurement of Mode Shapes of a Car Bonnet", Applied Mechanics and Materials Vol. 70 (2011) 45-50

18 DIC Lampeas, G., Pasialis, V., Siebert Th., Feligiotti, M., Pipino A., "Validation of impact simulations of a car bonnet by full-field optical measurements", Applied Mechanics and Materials Vol. 70 (2011) 51-56

12.2. TSA

1 TSA Greene, R.J., Patterson, E.A., Rowlands, R.E., 2008, 'Thermoelastic stress analysis', in *Handbook of Experimental Mechanics* edited by W.N. Sharpe Jr., Springer, New York.

2 TSA Dulieu-Barton, J., Stanley, P., "Development and applications of thermoelastic stress analysis", *Journal of Strain Analysis*, 33 (2), 93-104, 1998.

3 TSA Dulieu-Barton, J., "Introduction to thermoelastic stress analysis", *Strain*, 35 (2), 35-40, 1999.

4 TSA Pitaressi, G., Patterson, E.A., "A review of the general theory of thermoelastic stress analysis", *J. Strain Analysis*, 38 (5), 405-417, 2003.

5 TSA Lesniak, J.R., Boyce, B.R., "A high speed differential thermography camera", *Proc. SEM Spring Conf. on Experimental Mechanics*, Baltimore, Maryland, 491-497, 1994.

6 TSA Mountain, D.S., Webber, J.M.B., "Stress pattern analysis by thermal emission (SPATE)", *Proc. Soc. Photo-opt. Inst. Eng.* 164, 134-146, 1978.

7 TSA Harwood, N., Cummings, W.M., "Frequency-domain analysis techniques developed for SPATE response signals", *Proc. SPIE*. 1084, 143-158, 1989.

8 TSA Dulieu-Smith, J.M., "Alternative calibration techniques for quantitative thermoelastic stress analysis", *Strain*, 31, 9-16, 1995.

9 TSA Stanley, P., Dulieu-Smith, J.M., "Devices for the experimental determination of individual stresses form thermoelastic data", *J. Strain Analysis*, 31, 53-63, 1996.

10 TSA Barone, S., Patterson, E.A., "The development of simultaneous thermo- and photo-elasticity for principal stress analysis", *Strain*, 35 (2), 57-65, 1999.

11 TSA Mountain, D.S., Cooper, G.P., "Thermal evaluation for residual stress analysis (TERSA) – a new technique for assessing residual stress", *Proc. SPIE*, 1084, 103-110, 1989.

12 TSA Wong, A.K., Dunn, S.A., Sparrow, J.G., "Residual stress measurement by means of the thermoelastic effect", *Nature*, 332, 613-615, 1988.

13 TSA Tomlinson, R.A., Olden, E.J., "Thermoelasticity for the analysis of crack tip stress fields – a review", *Strain*, 35 (2), 49

14 TSA Potter, R.T., Greaves, L.J., "The application of thermoelastic stress analysis techniques to fibre composites", *Proc. SPIE*, 817, 134-146, 1987.

15 TSA Dulieu-Barton, J.M., Stanley, P., "Applications of thermoelastic stress analysis to composite materials", *Strain*, 35 (2), 41-48, 1999.

12.3. DSPI

1 DSPI Jones R., and Wykes C., Holographic and Speckle Interferometry, 2nd ed., Cambridge University Press, Cambridge, 1989

2 DSPI Sirohi, R.S., ed., *Speckle Metrology*, M. Dekker Inc., New York, 1993

3 DSPI Rastogi, P.K. (2001) Digital Speckle Pattern Interferometry and Related Techniques, John Wiley & Sons, Inc., New York

4 DSPI Wang, W.-C., Hwang, C.H., and Lin, S.Y., "Vibration measurement by the time-averaged electronic speckle pattern interferometry methods", Appl. Opt. 35 (1996) 4502-4509

5 DSPI Moore A.J., Hand D.P., Barton J.S., and Jones J.D.C., "Transient deformation measurement with electronic speckle pattern interferometry and a high-speed camera", Appl. Opt. Vol. 38, pp. 1159-62, 1999

6 DSPI Yang L.X., Siebert Th., "Digital Speckle Pattern Interferometry in Engineering", chapter 22 on "New Directions in Holography and Speckles", Ed. H. John Caulfield and Chandra S. Vikram Publisher American Scientific Publishers, ISBN 1-58883-101-9, pp 405-440(2008)

7 DSPI Hack, E., Feligiotti, M., Lampeas, G., Siebert, Th., Pipino, A., Ihle, A., "Assessment of impact damage in CFRP by combined thermal and speckle methods", Proceedings of the SPIE, Vol. 7387, 73870H-73870H-8 (2010)

8 DSPI Feligiotti, M.; Hack, E.; Lampeas, G.; Wang, W.; Mottershead, J. E.; Burguete. R. Use of integrated simulation and experimentation to quantify impact damage Applied Mechanics and Materials Vol. 70 (2011) 51-56